Pulmonary Epithelium Is a Prominent Source of Proteinase-activated Receptor-1–inducible CCL2 in Pulmonary Fibrosis

Paul F. Mercer[1]*, Robin H. Johns[1]*, Chris J. Scotton[1]*, Malvina A. Krupiczojc[1], Melanie Königshoff[2], David C. J. Howell[1], Robin J. McAnulty[1], Anuk Das[3], Andrew J. Thorley[4], Terry D. Tetley[4], Oliver Eickelberg[2], and Rachel C. Chambers[1]

[1]Centre for Respiratory Research, University College London, London, United Kingdom; [2]Justus Liebig University of Giessen, Giessen, Germany; [3]Centocor, Inc., Radnor, Pennsylvania; and [4]National Heart and Lung Institute, Imperial College London, London, United Kingdom

Rationale: **Studies in patients and experimental animals provide compelling evidence of the involvement of the major thrombin receptor, proteinase-activated receptor-1 (PAR_1), and the potent chemokine, chemokine (CC motif) ligand-2 (CCL2)/monocyte chemotactic protein-1, in the pathogenesis of idiopathic pulmonary fibrosis (IPF). PAR_1 knockout mice are protected from bleomycin-induced lung inflammation and fibrosis and this protection is associated with marked attenuation in CCL2 induction.**

Objectives: **The aim of this study was to determine which cell types represent the major source of PAR_1-inducible CCL2 in the fibrotic lung.**

Methods: **Using immunohistochemistry and dual immunofluorescence, we examined PAR_1 and CCL2 expression in the bleomycin model and human IPF lung. PAR_1 and CCL2 gene expression was also assessed in laser-captured alveolar septae from patients with IPF. The ability of PAR_1 to induce CCL2 production by lung epithelial cells was also examined *in vitro*.**

Measurements and Main Results: **We report for the first time that PAR_1 and CCL2 are coexpressed and co–up-regulated on the activated epithelium in fibrotic areas in IPF. Similar observations were found in bleomycin-induced lung injury. Furthermore, we show that thrombin is a potent inducer of CCL2 gene expression and protein release by cultured lung epithelial cells via a PAR_1-dependent mechanism.**

Conclusions: **These data support the notion that PAR_1 activation on lung epithelial cells may represent an important mechanism leading to increased local CCL2 release in pulmonary fibrosis. Targeting PAR_1 on the pulmonary epithelium may offer a unique opportunity for therapeutic intervention in pulmonary fibrosis and other inflammatory and fibroproliferative conditions associated with excessive local generation of thrombin and CCL2 release.**

Keywords: pulmonary fibrosis; IPF; epithelium; PAR; CCL2

AT A GLANCE COMMENTARY

Scientific Knowledge on the Subject

Studies in patients and experimental animals have provided evidence of the involvement of the major thrombin receptor, proteinase-activated receptor-1 (PAR_1), and the potent chemokine, chemokine (CC motif) ligand-2 (CCL2)/monocyte chemotactic protein-1, in the pathogenesis of pulmonary fibrosis.

What This Study Adds to the Field

This study shows that PAR_1 and CCL2 are coexpressed and co–up-regulated on the activated epithelium in idiopathic pulmonary fibrosis and the bleomycin model. PAR_1 ligation-induces CCL2 release by cultured lung epithelial cells *in vitro*. These data implicate the pulmonary epithelium as an important source of PAR_1-inducible CCL2 in idiopathic pulmonary fibrosis.

Increased local procoagulant activity is a characteristic feature of several chronic fibrotic lung conditions, including idiopathic pulmonary fibrosis (IPF), pulmonary fibrosis associated with systemic sclerosis, as well as acute conditions associated with excessive fibroproliferation, such as acute respiratory distress syndrome (ARDS) (reviewed in Reference 1). The pathophysiological significance of increased procoagulant activity in the fibroproliferative response to lung injury is supported by the observation that interventions targeting the coagulation cascade, with either direct thrombin inhibitors (2) or administration of activated protein C (3), nebulized heparin (4), or tissue factor pathway inhibitor gene transfer (5) substantially attenuate experimentally induced pulmonary inflammation and/or fibrosis.

The mechanisms by which the coagulation cascade drives lung inflammation and fibrosis in these models is still not fully understood, although they may not be dependent on the generation of fibrin, because fibrinogen knockout mice are not protected from lung fibrosis (6). In contrast, evidence supports an important role for thrombin and other coagulation proteinases acting via the proteolytic activation of the major high-affinity thrombin signaling receptor, proteinase-activated receptor-1 (PAR_1) (7). The pathological relevance of PAR_1 is supported by the observation of increased local PAR_1 expression in fibrotic foci in IPF and pulmonary fibrosis associated with systemic sclerosis (7, 8) but also in other fibrotic conditions, including those of the kidney (9) and the liver (10). In the context of experimental lung fibrosis, we have previously reported that PAR_1 deficiency affords protection from bleomycin-induced lung inflammation and fibrosis in mice (7). This protection is associated with reduced lung levels of the CC chemokine, chemokine (CC motif) ligand-2 (CCL2)/monocyte chemotactic protein (MCP)-1/JE, consistent with the notion that PAR_1 activation promotes the local generation of CCL2 in response to fibrotic lung injury.

(*Received in original form December 14, 2007; accepted in final form December 4, 2008*)

*These authors contributed equally to this article.

Supported by funding from the Medical Research Council (UK) (R.H.J.), the Wellcome Trust (program grant no. GR071124MA) (C.J.S.), and Centocor, Inc. (P.F.M.).

Correspondence and requests for reprints should be addressed to Rachel C. Chambers, Ph.D., Centre for Respiratory Research, University Street, London WC1E 6JJ, UK. E-mail: r.chambers@ucl.ac.uk

Am J Respir Crit Care Med Vol 179. pp 414–425, 2009
Originally Published in Press as DOI: 10.1164/rccm.200712-1827OC on January 22, 2009
Internet address: www.atsjournals.org

CCL2 is a potent mononuclear cell chemoattractant, expressed by numerous cell types, including monocytes/macrophages, fibroblasts, and epithelial cells (11), and CCL2 expression is increased in the lungs of patients with IPF (12). In addition to its ability to promote inflammation, CCL2 may also directly influence fibrosis via a number of mechanisms, including its ability to influence fibrocyte recruitment (13). Mice deficient for the major CCL2 receptor, chemokine (CC motif) receptor-2 (CCR2), are protected from bleomycin- and fluorescein isothiocyanate–induced lung fibrosis (14, 15) and anti-CCL2 gene therapy attenuates bleomycin-induced fibrosis (16). Serum CCL2/MCP-1 levels have been shown to correlate with the clinical course of interstitial lung disease treated with corticosteroid therapy, so that serum CCL2 levels may serve as a useful biomarker for disease progression (17). Bronchoalveolar lung fluid CCL2 levels also correlate with the severity of lung injury in ARDS (18), further supporting the notion that CCL2 is causally linked to the development of human fibroproliferative lung disease.

Widespread epithelial injury is fundamental to the development of these fibroproliferative lung disorders. The resultant aberrant repair process is thought to lead to the emergence of hyperplastic and proliferating epithelial cells, which are key pathological features in the lungs of patients with IPF (19) and ARDS (20), and also in the bleomycin model (21, 22). There is further good evidence that activated epithelial cells represent a major source of a range of proinflammatory and profibrotic mediators, including CCL2 (12). Tissue factor, the main initiator of the extrinsic pathway of coagulation, is also highly upregulated on type II pneumocytes and to some extent on alveolar macrophages, in close association with fibrin deposits in the lungs of patients with IPF and systemic sclerosis (23). Prominent tissue factor staining on alveolar epithelial cells has also been reported in ARDS (24). The alveolar epithelium is therefore likely to play an important role in the initiation of intraalveolar coagulation in response to both acute and chronic lung injury. Moreover, these cells may also signal in response to coagulation proteinases locally activated on the alveolar epithelium. In support of this notion, human cultured alveolar epithelial cell lines have been shown to express PAR_1 *in vitro* (25).

In light of the compelling evidence for PAR_1 and CCL2 in fibrotic lung disease, the aim of this study was to identify the major cell types responsible for PAR_1-inducible CCL2 in the fibrotic lung, focusing in particular on the potential contribution of the lung epithelium, a major site of CCL2 expression in IPF (12). Using immunohistochemistry and gene expression studies of laser-captured alveolar septae, we report for the first time that PAR_1 and CCL2 expression is increased on the alveolar and bronchial epithelium in pulmonary fibrosis. Macrophages were also dual immunoreactive for PAR_1 and CCL2 in IPF but also in control lung tissue. In contrast, spindle-shaped fibroblasts within fibrotic areas in IPF were strongly positive for PAR_1 but were only weakly positive for CCL2. We further report that thrombin is a potent inducer of CCL2 gene expression and protein release by cultured human lung epithelial cells via a PAR_1-dependent mechanism. The stimulatory effects of thrombin on CCL2 release were confirmed in freshly isolated primary human and murine alveolar epithelial cells. These data are consistent with the notion that activation of PAR_1 on the pulmonary epithelium may represent an important mechanism leading to increased local CCL2 release in the lungs of patients with IPF. Targeting PAR_1 on these cell types may offer promise for therapeutic intervention in pulmonary fibrosis, and potentially other inflammatory and fibroproliferative conditions associated with excessive local generation of thrombin and CCL2 release. We declare that some of this work has previously been published in abstract form (*see* References 26, 27).

METHODS

Materials

Human- and mouse-specific PAR_1 antibodies were a generous gift from E. Mackie (University of Melbourne, Melbourne, Australia). Both were raised in rabbits and purified by affinity chromatography. Human-specific antibodies were directed against amino acid residues 26–99 of human PAR_1 (anti-TRED) and mouse-specific PAR_1 antibodies were directed against the peptide SFFLRNPSENTFELVPL-NH_2 (anti-SFFL). Human-specific CCL2 antibodies (MAB2791) were obtained from R&D Systems (Oxon, UK) and mouse-specific CCL2 antibodies (sc-1784) were obtained from Santa Cruz Biotechnology (Santa Cruz, CA). 4′,6-Diamidino-2-phenylindole (D9564) was obtained from Sigma-Aldrich (Poole, UK), and goat anti-rabbit Alexa Fluor 555 (A31629) and goat anti-mouse Alexa Fluor 488 (A21151) were obtained from Invitrogen (Paisley, UK). The specific PAR_1 agonist TFLLR peptide and FTLLR partial-reverse control peptide were synthesized as amidated peptides by R. Mecham (University of Washington, St. Louis, MO). A549 cell lines were obtained from the American Type Culture Collection (ATCC, Manassas, VA) via LGC Promochem (Middlesex, UK). The PAR_1 antagonist RWJ-58259 was kindly provided by C. Derian (Johnson & Johnson Pharmaceutical R&D, Philadelphia, PA). The PAR_1–$G\alpha_q$-specific allosteric inhibitor Q94 was kindly provided by A. Gilchrist (Caden Biosciences, Madison, WI). Paired antibodies MAB679 and BAF279 for the human CCL2 ELISA were obtained from R&D Systems; and human recombinant CCL2 protein standard was from Peprotech (Rocky Hill, NJ).

Bleomycin Animal Model of Lung Injury

Mice were housed in a specific pathogen–free facility and used when between 6 and 8 weeks of age, in accordance with the UK Home Office Animals (Scientific Procedures) Act, 1986. Bleomycin (Nippon Kayaku Co. Ltd., Tokyo, Japan) or saline was administered by single intratracheal injection (1 mg/kg body weight in 50 μl of saline) into a surgically exposed trachea under anesthesia. Mice were killed on Day 6. The trachea was cannulated, and lungs were insufflated with 4% paraformaldehyde in phosphate-buffered saline (PBS) at a pressure of 20 cm H_2O, followed by removal of the heart and inflated lungs *en bloc* and immersion for 4 hours in fresh fixative. Subsequently lungs were transferred into 15% sucrose in PBS and left overnight at 4°C, before transfer to 70% ethanol.

Human Subject Details

For histologic analyses, fibrotic lung tissue was removed from two individuals diagnosed as having IPF, with histologic evidence of usual interstitial pneumonia, undergoing transplant surgery. Control tissue was derived from the lungs of patients undergoing lobectomy for removal of a primary lung tumor, which showed no histologic evidence of disease. Tissue was taken from an area distal to the resected primary tumor. All tissue was obtained with the approval of the joint University College London/University College London Hospital (London, UK) and Brompton Hospital (London, UK) ethics committees.

Lung tissue biopsies for laser microdissection (Giessen cohort) were obtained from a total of 10 patients with IPF (usual interstitial pneumonia pattern; mean age, 51.3 ± 11.4 yr; 4 females and 6 males) and 10 control subjects (organ donors; mean age, 47.5 ± 13.9 yr; 5 females and 5 males). The study protocol was approved by the Ethics Committee of the Justus Liebig University School of Medicine (Giessen, Germany) (AZ 31/93). Informed consent was obtained for each subject for the study protocol.

Histologic Analysis

Individual lobes of mouse lungs or human biopsy material were placed in processing cassettes, dehydrated through a serial alcohol gradient, and embedded in paraffin wax blocks. Before immunostaining, 4-μm-thick lung tissue sections were dewaxed in xylene, rehydrated through decreasing concentrations of ethanol, and washed in PBS.

Immunohistochemistry

For serial section studies, human and mouse PAR_1 antigens were unmasked by microwaving sections in 10 mM citrate buffer, pH 6.0 (twice for 10 min); human CCL2 antigens were unmasked by in-

cubating with proteinase K (20 μg/ml), in 10 mM TRIS−5 mM ethylenediaminetetraacetic acid buffer (pH 7.4), for 10 minutes at room temperature. No treatment was required for unmasking murine CCL2 antigens. Immunostaining was undertaken by the avidin–biotinylated enzyme complex method (Vector Laboratories, Burlingame, CA) with antibodies against human PAR_1 (anti-TRED; 3 μg/ml), mouse PAR_1 (anti-SFFL; 0.14 μg/ml), human CCL2 (MAB2791; final concentration, 8 μg/ml; R&D Systems), or mouse CCL2 (sc-1784; final concentration, 0.5 μg/ml; Santa Cruz Biotechnology), and equivalent concentrations of polyclonal nonimmune IgG controls. After incubation with an appropriate biotin-conjugated secondary antibody and subsequently with streptavidin–horseradish peroxidase solution (each at 1:200 dilution to a final concentration of 4.2 μg/ml; Dako, Glostrup, Denmark), color development was performed with 3,3′-diaminobenzidine tetrachloride (Vector Laboratories) as a chromogen. Sections were counterstained with Gill-2 hematoxylin (Thermo-Shandon, Pittsburgh, PA), dehydrated, and mounted. The specificity of the signal obtained was confirmed by showing that no positive staining was detectable when the primary antibody was substituted with an equivalent concentration of nonimmune IgG. For dual immunofluorescence studies, PAR_1 and CCL2 antigens were unmasked by incubating with proteinase K (40 μg/ml), in 10 mM TRIS−5 mM ethylenediaminetetraacetic acid buffer (pH 7.4), for 10 minutes at room temperature. Tissue sections were subsequently incubated with the antibodies against human PAR_1 and human CCL2 as outlined previously. Sections were then incubated with goat anti-rabbit Alexa Fluor 555 (specific for α-TRED), followed by goat anti-mouse Alexa Fluor 488 (specific for MAB2791), and finally 4′,6-diamidino-2-phenylindole (0.5 μg/ml) for visualization of nuclei. For light microscopy, sections were examined with an Olympus BX40 light microscope. For immunofluorescence sections were examined with an immunofluorescence microscope (Axioskop 2; Zeiss, Welwyn Garden City, UK) equipped with Zeiss filter sets 02 (blue), 15 (red), and 09 (green). Images were captured and analyzed with a QICAM FAST1394 CCD camera from Qimaging, Inc. (Surrey, BC, Canada) and QCAPTURE Pro software (Qimaging, Inc.).

Laser-capture Microdissection

Microdissection was performed as described previously (28). In brief, 10-μm cryosections were mounted on glass slides, stained with hemalaun for 45 seconds, immersed in 70% and 96% ethanol, and stored in 100% ethanol until use. Alveolar septae were selected and microdissected with the Laser Microbeam System (PALM; Zeiss, Bernried, Germany). Microdissected tissues were then transferred into reaction tubes containing 200 μl of RNA lysis buffer and samples were processed for RNA analysis, as described later.

Isolation of Primary Human and Murine Epithelial Cells

Primary human alveolar epithelial type II (ATII) cells were isolated from lungs of grossly normal appearance after resection for lung carcinoma, with the approval of the Royal Brompton and Harefield Ethics Committee, as previously described (29). Lung tissue was perfused and inflated with 0.25% trypsin in Hanks' balanced salt solution (Sigma-Aldrich) and incubated at 37°C for 45 minutes; trypsin was replaced twice during this time. The tissue was finely chopped in the presence of newborn calf serum (Invitrogen). The chopped tissue was then incubated with DNase (250 μg/ml; Sigma-Aldrich) and the mixture was passed through 300-μm and then 40-μm filters to remove large tissue debris. The cell suspension was centrifuged (290 × *g*, 10 min, 20°C) and the resulting pellet was resuspended in DCCM-1 medium (Biological Industries, Kibbutz Beit Haemek, Israel) containing DNase (50 μg/ml). Cells were incubated in tissue culture flasks for 2 hours at 37°C in a humidified incubator to allow differential adherence of contaminating mononuclear cells. Nonadherent ATII cells in suspension were removed and centrifuged. The cell pellet was resuspended in DCCM-1 supplemented with 10% fetal calf serum, penicillin–streptomycin, and L-glutamine and seeded at a density of 1×10^6 ATII cells per well in 12-well plates. Cells were characterized by staining for alkaline phosphatase, and expression of surfactant proteins A and C as previously described (27). Cells reached confluence by 48 hours.

Primary murine ATII cells were isolated from mice as previously described (30). In brief, lungs were lavaged with 1 ml of sterile PBS and tissues were digested with dispase and minced. The suspension was sequentially filtered through 100-, 20-, and 10-μm nylon meshes and centrifuged at 200 × *g* for 10 minutes. The pellet was resuspended in Dulbecco's modified Eagle's medium and a negative selection for lymphocytes/macrophages was performed by incubation on CD16/32- and CD45-coated Petri dishes for 30 minutes at 37°C.

Negative selection for fibroblasts was performed by adherence for 45 minutes on cell culture dishes. Cell purity was routinely assessed by epithelial cell morphology and immunofluorescence analysis of pan-CK (cytokeratin) and pro-SPC (surfactant protein C) (both positive), and SMA (smooth muscle α-actin) and CD45 (both negative). Cell viability was checked by trypan blue exclusion. The ATII cells used demonstrated 95 ± 3% purity and greater than 97% viability. Finally, ATII cells were suspended in Dulbecco's modified Eagle's medium plus 10% fetal calf serum, penicillin–streptomycin, and L-glutamine and cultured in a humidified atmosphere of 5% CO_2 at 37°C.

Epithelial Cell Line Culture

A549 cells (ATCC) were maintained in F12K (Invitrogen) and BEAS-2B cells were maintained in RPMI 1640 (Invitrogen), all supplemented with 10% fetal calf serum, penicillin–streptomycin, and L-glutamine, until confluence in a humidified atmosphere of 5% CO_2 at 37°C. Cells were grown in 6- or 12-well plates until confluency, at which point they were quiesced for 24 hours in serum-free basic medium without supplements before their use in experiments.

Quantitative Real-time Polymerase Chain Reaction

Total RNA was isolated from cultured cell monolayers or microdissected lung, using TRIzol reagent according to the manufacturer's protocol (Invitrogen). After DNase treatment with DNA-*free* (Applied Biosystems/Ambion, Austin, TX), 1 μg of RNA was used to synthesize single-stranded cDNA, using an RNA PCR core kit (Applied Biosystems, Foster City, CA). Quantitative real-time polymerase chain reaction (qPCR) was then performed with Platinum SYBR Green qPCR Supermix (Invitrogen, Carlsbad, CA) with forward and reverse primers at a final concentration of 500 nM. For A549-derived samples PCR was conducted with a Roche LightCycler 1.5 and analyzed with LightCycler Software 3.5 (Roche Applied Science, Sussex, UK). For laser-capture microdissected samples, qPCR was performed with an Applied Biosystems sequence detection system 7700 (Applied Biosystems). Cycling conditions were as follows: 2 minutes at 50°C (one cycle), 2 minutes at 95°C (one cycle); then 5 seconds at 95°C, 5 seconds at 55°C, and 15 seconds at 72°C (45 cycles). For each gene, crossing point (Cp) values were determined from the linear region of the logarithmic amplification plot and normalized by subtraction of the Cp value for 18S or hypoxanthine phosphoribosyltransferase as appropriate (generating a ΔCp value). Relative change was determined by subtraction of the ΔCp value for the control sample from the ΔCp value for the stimulated/fibrotic sample (ΔΔCp value). Fold change was subsequently calculated according to the formula $2^{-\Delta\Delta Cp}$ (where ΔΔCp was converted to an absolute value). The specificity of the products obtained by PCR was confirmed by melting curve analysis and gel electrophoresis. Primers used are outlined in Table 1.

Human CCL2 ELISA

Each well of a 96-well ELISA plate was coated with 50 μl of 2-μg/ml MAB679 (R&D Systems) in bicarbonate coating buffer, left for 5 hours at room temperature, and then washed. One hundred microliters of PBS−1% bovine serum albumin was added to each well and the plate was left overnight at 4°C. Fifty microliters of either CCL2 standard or sample was added, and the plate was incubated for 2 hours at room temperature. After washing, 50 μl of 100-ng/ml BAF279 (R&D Systems) was added to each well, and left for 2 hours at room temperature. The plate was washed, and 50 μl of a 2-μg/ml dilution of streptavidin–horseradish peroxidase (Dako) was added for 30 minutes. After washing, 50 μl of 3,3′,5,5′-tetramethylbenzidine substrate (BD Biosciences, San Diego, CA) was added to each well. After 30 minutes, color development was quenched with 0.19 M H_2SO_4, and absorbances were measured on a plate reader at 450 nm.

Statistical Analysis

Statistical analysis was performed with GraphPad Prism software (GraphPad Software, San Diego, CA). All differences in mRNA levels

TABLE 1. QUANTITATIVE RT-PCR PRIMER PAIRS

Gene	Forward Primer	Reverse Primer
hCCL2	5′-AGCAAGTGTCCCAAAGAAGC-3′	5′-CATGGAATCCTGAACCCACT-3′
$hPAR_1$	5′-CCATCGTTGTGTTCATCCTG-3′	5′-GACCCAAACTGCCAATCACT-3′
h18S	5′-TTGACGGAAGGGCACCACCAG-3′	5′-GCACCACCACCCACGGAATCG-3′
hHPRT	5′-GGCTTTGTATTTTGCTTTTCCA-3′	5′-AAGGACCCCACGAAGTGTTG-3′

Definition of abbreviations: hCCL2 = chemokine (CC motif) ligand-2; HPRT = hypoxanthine phosphoribosyltransferase; PAR_1 = proteinase-activated receptor-1.

compared differences in ΔCp values. Differences in mRNA levels between donor and IPF microdissected alveolar septae were evaluated by two-tailed Student *t* test of equal variance. Paired comparisons of fold change of mRNA levels in response to thrombin or TFLLR and relative to their time point–matched control were also evaluated by Student *t* test. Comparison of more than two groups was evaluated by one-way analysis of variance (ANOVA) with the Student-Newman-Keuls method for post-hoc pair-wise comparisons. Comparison of the overall difference in CCL2 protein release between thrombin and control over a time course, and of subsequent differences at each time point, was evaluated by two-way ANOVA. A *P* value less than 0.05 was considered significant.

RESULTS

PAR_1 and CCL2 Immunolocalization after Bleomycin-induced Lung Injury

Epithelial cells have previously been reported to strongly express CCL2 in fibroproliferative lung disease (12). We have previously reported that protection from bleomycin-induced pulmonary inflammation and fibrosis in $PAR_1^{-/-}$ mice is associated with reduced lung levels of CCL2 (7). To determine the potential cellular sources of PAR_1-inducible CCL2 in the fibrotic lung, we examined serial lung sections of wild-type mice for CCL2 and PAR_1 immunoreactivity, 6 days after bleomycin challenge. Saline-instilled control mice displayed weak PAR_1 and CCL2 immunostaining, confined to the bronchial epithelium (Figures 1A and 1B). In contrast, areas of bleomycin-injured lungs displaying both moderate (Figures 1C and 1D) and severe damage (Figures 1E and 1F) showed intense PAR_1 and CCL2 signals associated with the alveolar and bronchial epithelium. Macrophages identifiable by their distinctive rounded morphology were also dual positive for PAR_1 and CCL2 in bleomycin-instilled mice (Figures 1C and 1D) and, although in fewer numbers, also in saline-instilled control mice (not shown in Figure 1).

PAR_1 and CCL2 Immunolocalization in Idiopathic Pulmonary Fibrosis

To determine whether these findings translate to human fibrotic lung disease we examined the immunolocalization of CCL2 and PAR_1 on serial sections from control and IPF lungs (Figure 2). To facilitate the identification of activated epithelial cells and macrophages in the grossly remodeled fibrotic lung, sections were immunostained with antibodies against the epithelial and macrophage markers CK7 and CD68, respectively (CK7, Figures 2A and 2B; CD68, Figures 2G and 2H). Figure 2 shows an area of

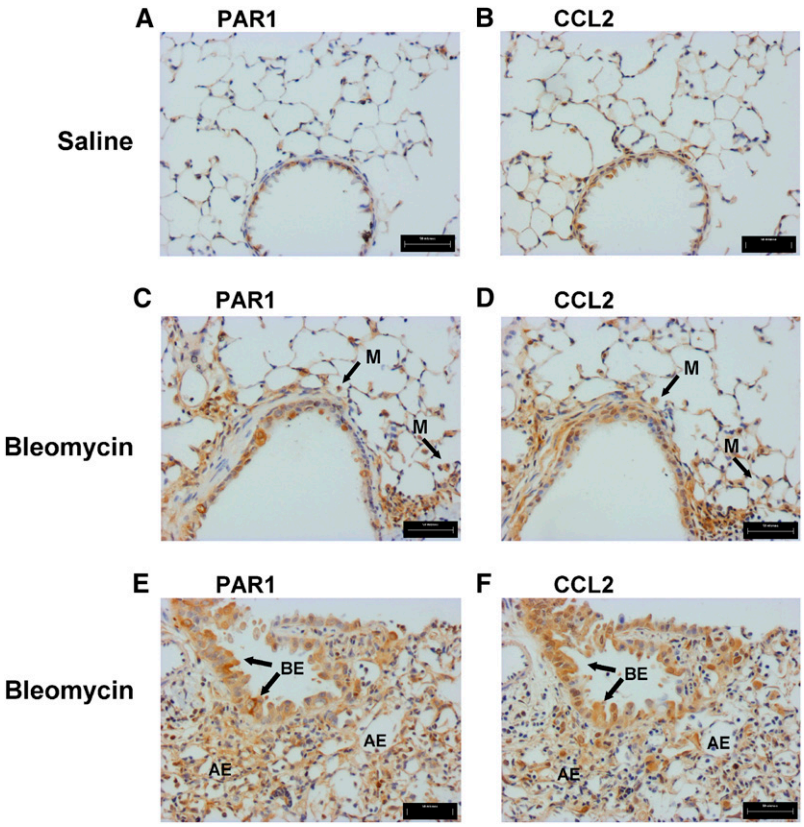

Figure 1. Proteinase-activated receptor-1 (PAR_1) and chemokine (CC motif) ligand-2 (CCL2) are coexpressed in bleomycin-induced lung injury. Shown is the immunohistochemical localization of PAR_1 (*A*, *C*, and *E*) and CCL2 (*B*, *D*, and *F*) in adjacent lung sections 6 days after instillation of saline (*A* and *B*) or bleomycin (*C*–*F*). Increased immunoreactivity for both PAR_1 and CCL2 was observed on bronchial epithelial cells (BE, *arrows*) and alveolar epithelial cells (AE) as well as macrophages (M) in both moderate (*C* and *D*) and severe (*E* and *F*) lesions. *Scale bars*: (*A*–*F*) 50 μm.

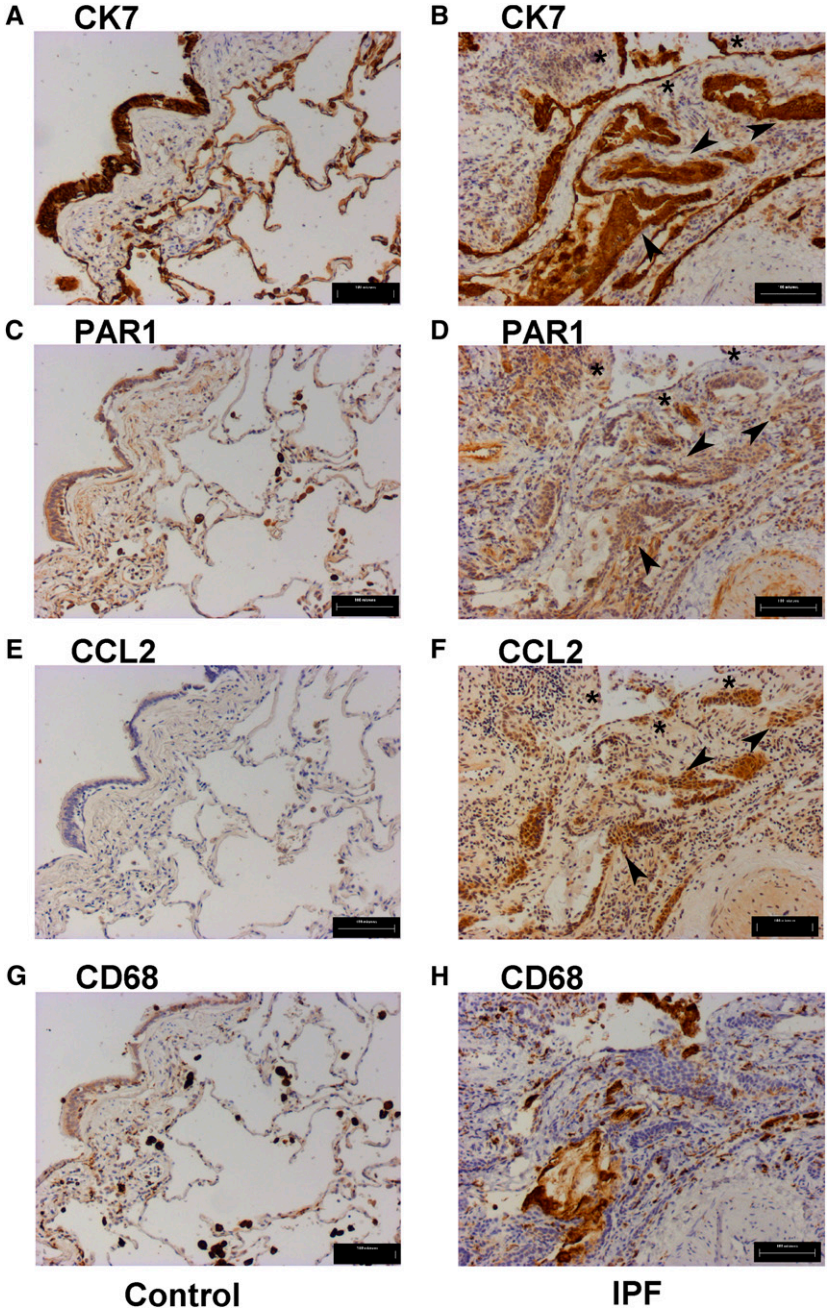

Figure 2. Proteinase-activated receptor-1 (PAR_1) and chemokine (CC motif) ligand-2 (CCL2) immunostaining in idiopathic pulmonary fibrosis (IPF) identifies epithelial cells and macrophages in fibrotic areas as major cell types displaying dual immunoreactivity. Shown is immunohistochemistry for the epithelial cell marker cytokeratin-7 (CK7) (*A* and *B*), PAR_1 (*C* and *D*), CCL2 (*E* and *F*), and CD68 (*G* and *H*), in serial sections of IPF (*right*) and control lung (*left*). Immunostaining for CCL2 (*F*), observed in discrete areas of the IPF lung, is associated with both the epithelial marker CK7 (*B*) and PAR_1 (*D*), most prominently on cells morphologically characteristic of hyperplastic alveolar (*asterisks*) and bronchial epithelium (*arrowheads*) (*B*, *D*, and *F*). PAR_1 and CCL2 staining is also evident in regions of macrophage infiltration demarcated by CD68 immunoreactivity (*D*, *F*, and *H*). Control human lung is immunoreactive for PAR_1 (*C*) in CK7-positive alveolar and bronchial epithelial cells (*A*). CCL2 staining is absent from all CK7-positive cells in control lung (*A* and *E*); however, weak expression is observed in CD68-positive cells morphologically characteristic of macrophages (*G*), which are positive for PAR_1 (*C*). *Scale bars*: (*A–H*) 100 μm.

active fibrosis within which discrete patches of cells, intensely immunoreactive for both PAR_1 and CCL2, are observed (Figures 2D and 2F). Staining within these areas was found to associate most commonly with cells strongly positive for the epithelial marker CK7 (Figure 2B). Although definitive characterization was difficult because of the grossly remodeled nature of the tissue, CK7/PAR_1/CCL2-positive cells were morphologically characteristic of both cuboidal bronchial (*arrowheads*) and hyperplastic alveolar epithelium (*asterisks*), bordering fibrotic foci. PAR_1 and CCL2 coexpression was also associated with CD68-positive macrophages (Figure 2H), as well as with CD68/CK7-negative cells with a morphology characteristic of smooth muscle cells and discrete fibroblasts within fibrotic areas. It is noteworthy, however, that whereas PAR_1 immunostaining on these CK7/CD68-negative mesenchymal cells was strong, CCL2 immunoreactivity was weak in comparison with the CK7-positive epithelium (Figures 2D and 2F). Blood vessel endothelial cells, which were also strongly positive for PAR_1 (Figure 2D), similarly lacked a convincing positive signal for CCL2 (Figure 2F).

By comparison, the control lung was found to exhibit more moderate PAR_1 immunostaining associated with CK7-positive cells, with the strongest signal localizing to both the alveolar and bronchial epithelium (Figures 2A and 2C). Intense PAR_1 immunostaining was consistently observed for CD68-positive macrophages (Figure 2G) and these cells were also positive for CCL2. In contrast to the IPF lung, there was no staining for CCL2 associated with any CK7-positive epithelial cells in control lungs (Figures 2A and 2E).

To consolidate our initial observations of serial sections with optimal preservation of lung architecture, we also performed dual immunofluorescence for PAR_1 and CCL2 in the IPF lung (Figure 3). A limitation of this technique is that antigen-unmasking treatments for PAR_1 and CCL2 differ considerably (PAR_1: heating in citrate buffer, pH 6, twice for 10 min; CCL2: proteinase

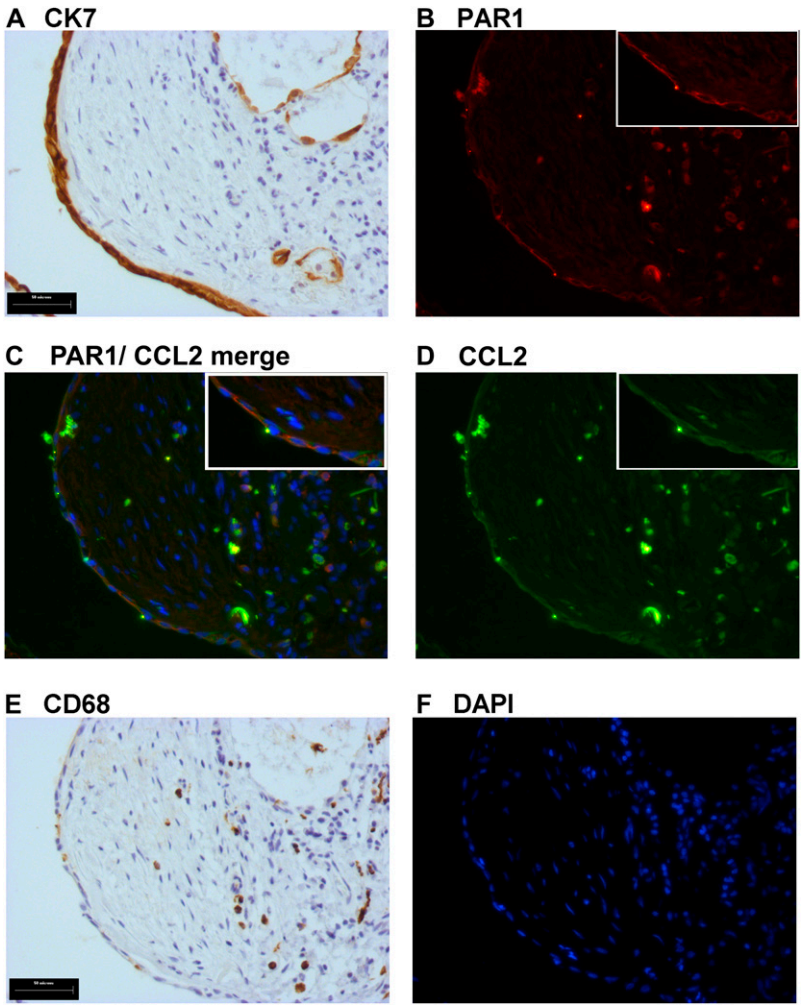

Figure 3. Dual immunofluorescence reveals coimmunostaining for proteinase-activated receptor-1 (PAR_1) and chemokine (CC motif) ligand-2 (CCL2) on epithelial cells overlying fibrotic foci and infiltrating macrophages. Immunohistochemistry for the epithelial cell marker cytokeratin-7 (CK7) (*A*) and the macrophage marker CD68 (*E*) in serial sections, directly adjacent to dual immunofluorescence costaining for PAR_1 and CCL2 (*C*). PAR_1-positive cells (*B*) are visualized in *red*, CCL2 (*D*) in *green*, and cells copositive for PAR_1 and CCL2 appear *orange* (*C*). Cell nuclei were visualized by 4′,6-diamidino-2-phenylindole (DAPI) staining (*F*, *blue*). Colocalization of PAR_1 and CCL2 is prominent on CK7-positive epithelial cells (*B* and *A*) overlying the fibrotic focus, in addition to infiltrating inflammatory cells positive for the macrophage antigen CD68 (*B* and *E*). *Scale bars*: (*A* and *E*) 50 μm.

K [20 μg/ml], 10 min at room temperature). The best compromise treatment (PAR_1 and CCL2 together: proteinase K [40 μg/ml], 10 min at room temperature), which enabled dual immunofluorescence staining to be performed, resulted in a reduced signal on cells strongly positive for CCL2 and PAR_1, with a loss of signal on cells that were weakly positive in serial sections. The strongest signal was observed for PAR_1 (Figure 3B, *red*) and CCL2 (Figure 3D, *green*) colocalized (Figure 3C [merge], *orange*) to CK7-positive epithelial cells overlying fibrotic foci (Figures 3A and 3C) and CD68-positive macrophages (Figures 3E and 3C).

Taken together, these studies led us to conclude that PAR_1 and CCL2 dual immunostaining is most prominently associated with the lung epithelium and macrophages in IPF, with the most consistent costaining observed in areas of fibrosis/fibrotic foci. Smooth muscle cells and fibroblast-like cells within fibrotic areas/foci were strongly positive for PAR_1 but the signal for CCL2 was relatively weak for these cell types. In the control lung, the pulmonary epithelium was positive for PAR_1 but not for CCL2; whereas macrophages were dual positive for both PAR_1 and CCL2.

PAR_1 and CCL2 mRNA Levels Are Increased in Microdissected Alveolar Septae in Patients with IPF

Our initial findings in murine and human IPF lung sections suggest that the activation of PAR_1 on the injured/activated epithelium could represent a potential cellular source of CCL2 in IPF. To begin to examine this hypothesis, we evaluated PAR_1 and CCL2 mRNA levels in microdissected alveolar septae from patients with IPF and the corresponding areas in control donor lung tissue by qPCR. The predominant epithelial phenotype of microdissected septae was confirmed by differential expression pattern analysis of a panel of markers, including CK, SPC, SPA, CD45, platelet–endothelial cell adhesion molecule (PECAM), vimentin, smooth muscle α-actin, and E-cadherin. Moreover, macrophages were actively identified and removed from microdissected areas. Using this approach, we show that PAR_1 and CCL2 transcripts were detectable at low levels in control donor lung septae, and that there is a marked increase in mRNA levels for both CCL2 ($P < 0.05$) and PAR_1 ($P < 0.005$, Student *t* test, two tailed, equal variance) in alveolar septae from patients with IPF (Figure 4). Taken together, these data demonstrate that PAR_1 and CCL2 mRNA levels are highly up-regulated in the alveolar epithelium of patients with IPF and support the notion that the epithelium might represent an important cellular source of PAR_1-inducible CCL2 in IPF.

PAR_1 Is Necessary and Sufficient for Thrombin-induced CCL2 Release by Cultured Lung Epithelial Cells

Disruption and reactive hyperplasia of the epithelium are major histopathologic features of the IPF lung. To examine the hypothesis that the epithelium might represent an important cellular source of PAR_1-inducible CCL2 in IPF, we examined whether activation of PAR_1 leads to the induction and release of CCL2 by cultured lung epithelial cells. Initial time-course and concentration–response experiments were performed with A549 cells, as a model cell type of type II alveolar epithelium, and with BEAS-2B cells,

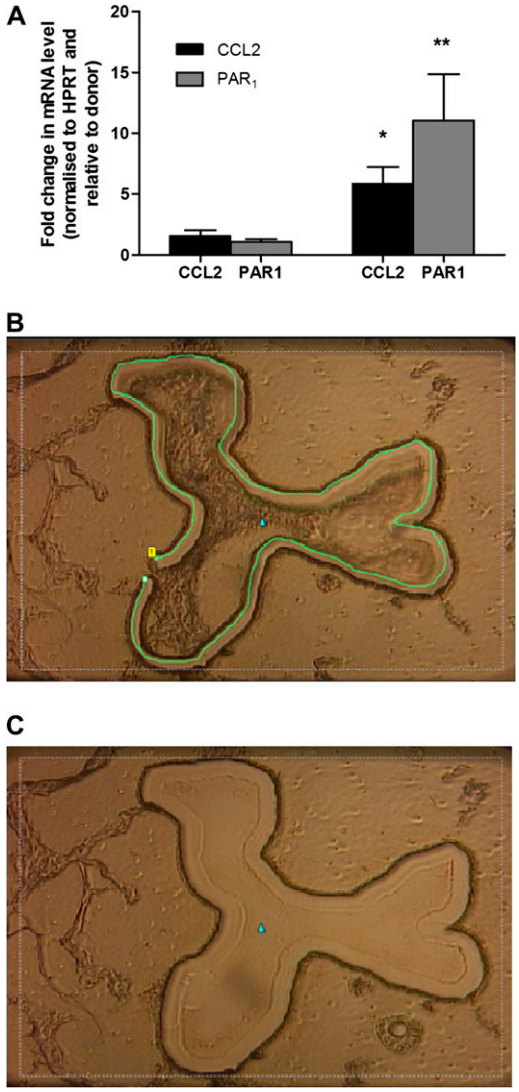

Figure 4. Proteinase-activated receptor-1 (PAR_1) and chemokine (CC motif) ligand-2 (CCL2) mRNA levels are increased in alveolar septae in idiopathic pulmonary fibrosis (IPF). (*A*) PAR_1 and monocyte chemotactic protein (MCP)-1 expression in microdissected alveolar septae from human IPF and donor lungs as analyzed by quantitative real-time polymerase chain reaction. Data are enumerated as the fold increase relative to mean mRNA levels in donors, normalized to the housekeeping gene hypoxanthine phosphoribosyltransferase (HPRT) ± SEM (patients with IPF: MCP-1, n = 8; PAR_1, n = 9) (donor subjects: MCP-1, n = 7; PAR_1, n = 6). *$P < 0.05$, **$P < 0.005$ (Student *t* test, two-tailed, two sample, equal variance). *B* and *C* show a typical example of an alveolar septum (*B*) before and (*C*) after microdissection.

representative of the bronchial epithelium. For all experiments, cells were serum-starved for 24 hours before incubation with either control medium or medium containing thrombin. CCL2 protein release into culture supernatants was quantified by ELISA. Time-course experiments with A549 cells, with a standard concentration of 10 nM thrombin, demonstrated that thrombin was a potent inducer of CCL2 release by these cells and that the time point of exponential induction between medium control and thrombin-stimulated cells was at 6 hours (Figure 5A). For subsequent concentration–response experiments, A549 cells were therefore exposed to thrombin for 6 hours. The results obtained (Figure 5B) showed that thrombin induced CCL2 protein release in a concentration-dependent manner from 0.1 nM onward, with values increased by about sixfold at 10 nM and ninefold at the highest thrombin concentration tested (100 nM). Interestingly, no plateau in CCL2 production was observed even at this high concentration of the proteinase. Basal accumulation of CCL2 also increased in unstimulated A549 cell supernatants over time, suggesting that CCL2 is constitutively expressed by these cells.

To determine the involvement of PAR_1 in the induction of thrombin-induced CCL2 release, A549 cells were exposed to the PAR_1-specific activating peptide TFLLR-NH_2 (TFLLR, 200 μM) or the same concentration of the inactive control peptide, FTLLR-NH_2 (FTLLR), for 6 hours (Figure 5C). The PAR_1-specific agonist induced a similar sixfold increase in CCL2 release ($P < 0.01$, one-way ANOVA), whereas the inactive control peptide had no effect, indicating that PAR_1 activation alone is sufficient for CCL2 release by these cells.

We next examined the effect of thrombin and TFLLR-NH_2 on A549 CCL2 mRNA levels over time. Both thrombin and TFLLR increased CCL2 mRNA levels in A549 cells (Figure 5C) and BEAS-2B (data not shown), with a peak in both cell types between 1.5 and 3 hours before a return to baseline values by 12 hours. Maximal increases in CCL2 mRNA levels in response to thrombin stimulation temporally preceded the observed increases in CCL2 protein release (Figures 5A and 5D).

To determine whether PAR_1 is necessary for thrombin-induced CCL2 expression we next examined the effect of the PAR_1-specific antagonist, RWJ-58259, on thrombin-induced CCL2 mRNA levels at 1.5 hours and on CCL2 protein release at 6 hours. The results obtained show that RWJ-58259 used at a concentration of 2 μM was sufficient to completely block thrombin-induced CCL2 expression both at the mRNA (Figure 5E) and protein levels (Figure 5F). The necessity for PAR_1 in mediating this response was also examined with the novel PAR_1 antagonist, Q94, which blocks PAR_1 signaling by allosterically blocking the interaction between PAR_1 and the $G\alpha_q$ subunit (31). Q94 at a concentration of 1 μM was sufficient to completely block thrombin-induced CCL2 protein release (Figure 5G), indicating that PAR_1-induced CCL2 production is mediated via PAR_1 coupling to $G\alpha_q$.

Evidence suggests that coagulation factor Xa (FXa) is also capable of exerting cellular responses by activating either PAR_1 or PAR_2, depending on cell type (32, 33). In contrast to thrombin, FXa, when used at concentrations sufficient to induce PAR_1 signaling in human lung fibroblasts (32), failed to significantly influence CCL2 mRNA levels in A549 cells (data not shown).

In addition to activating PAR_1, thrombin is also capable of signaling via PAR_4 and A549 cells have previously been shown to respond to PAR_4 activation *in vitro* (25). We therefore also examined the effect of the potent PAR_4 agonist peptide, AYPGKF (34) on CCL2 gene expression in A549 cells. No CCL2 induction was observed under the experimental conditions employed in this study; moreover these cells were found to be negative for PAR_4 expression at the mRNA level (data not shown).

Although IPF is considered primarily a parenchymal disease, peribronchial fibrosis with associated epithelial hyperplasia and bronchiolization is commonly observed in patients with IPF (35). Our immunolocalization studies revealed that the bronchial epithelium in the highly distorted IPF lung is also dual immunopositive for PAR_1 and CCL2. We therefore also examined the effect of thrombin on CCL2 release by the bronchial epithelial cell line BEAS-2B (Figure 5H) (36). These cells responded strongly to thrombin stimulation and RWJ-58259 completely blocked thrombin-induced CCL2 mRNA levels and protein production.

To validate the observations obtained with epithelial cell lines, limited confirmatory experiments were also performed

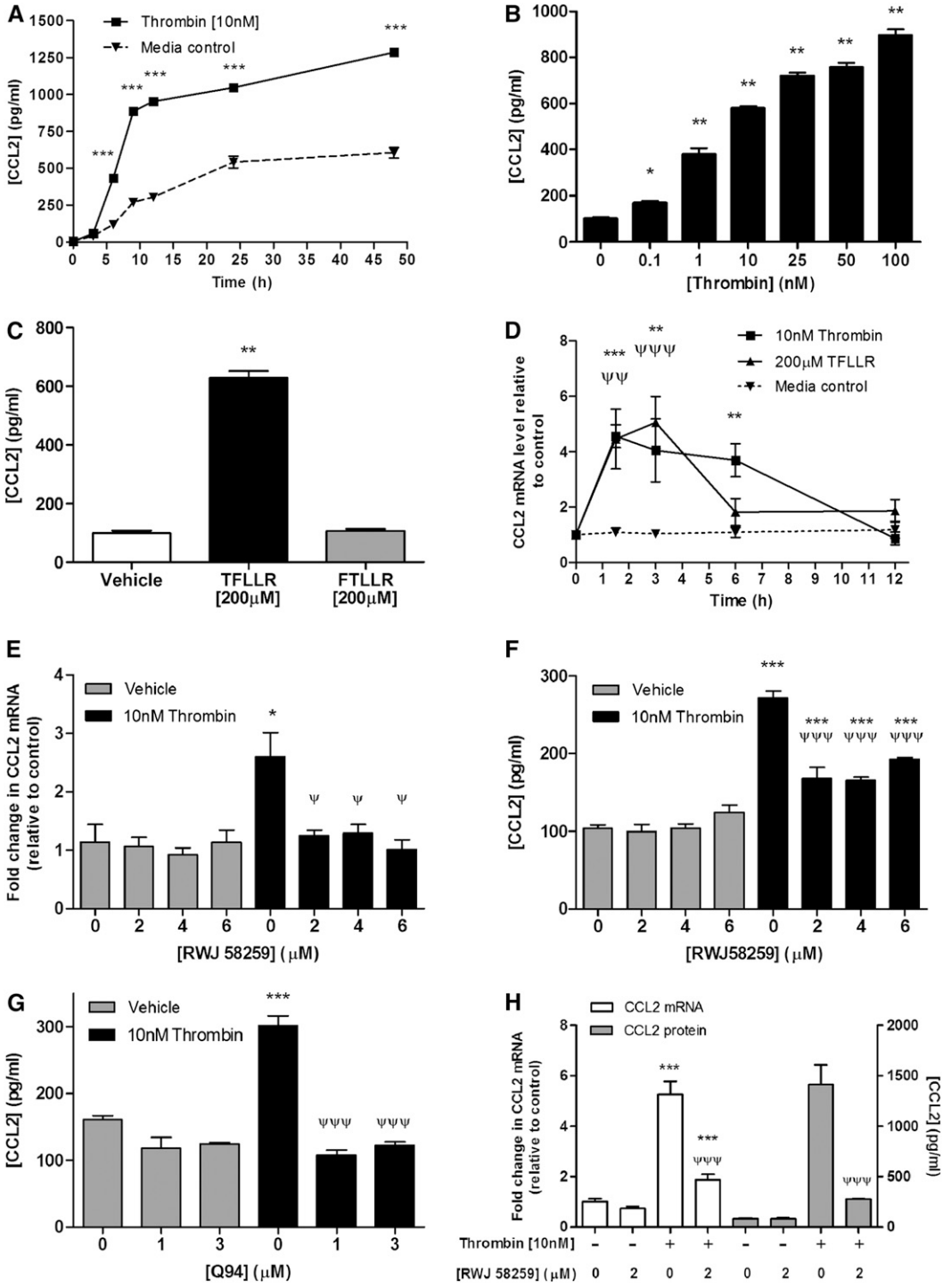

Figure 5. Thrombin induces chemokine (CC motif) ligand-2 (CCL2) release by lung epithelial cells via a proteinase-activated receptor-1 (PAR_1)-dependent mechanism. (*A*) Time course for the effect of thrombin on CCL2 protein release by A549 cells. Cells were exposed to serum-free control medium (F12K) or thrombin (10 nM) for incubation times from 3 to 48 hours, supernatants were collected, and CCL2 protein release was measured by ELISA. $^{***}P < 0.001$, post-hoc pair-wise comparison of thrombin and medium control groups at each time point (two-way analysis of variance [ANOVA] with Bonferroni post-hoc testing). (*B* and *C*) Effect of PAR_1 activation on CCL2 protein release by A549 cells. Cells were exposed to serum-free control medium, thrombin (0.1 to 100 nM) (*B*), the PAR_1-activating peptide TFLLR-NH_2 (200 μM) (*C*), or the inactive partial reverse peptide FTLLR-NH_2 (*C*) for 6 hours. Cell supernatants were analyzed for CCL2 protein release by ELISA. Data represent the mean ± SEM of four replicates per group. $^{*}P < 0.05$, $^{**}P < 0.01$, comparison of thrombin or TFLLR-NH_2 treatment with medium control (one-way ANOVA with Student-Newman-Keuls post-hoc testing). (*D*) Time course for the effect of thrombin and TFLLR-NH_2 on CCL2 mRNA levels. A549 cells were exposed to serum-free control medium (F12K), thrombin (10 nM), or TFLLR-NH_2 (200 μM) for incubation times from 1.5 to 12 hours. CCL2 mRNA levels at each time point were assessed by quantitative real-time polymerase chain reaction (qPCR). Data are expressed as fold change relative to time 0 for each time point after normalization to 18S RNA. Data represent the mean ± SEM of four replicates per group at each time point. $^{**}P < 0.01$, $^{***}P < 0.001$, comparison of thrombin-induced change in crossing point (ΔCp) with time point–matched control; $^{\Psi\Psi}P < 0.01$, $^{\Psi\Psi\Psi}P < 0.001$, comparison of TFLLR-induced mRNA levels with time point–matched control (two-way ANOVA with Bonferroni post-hoc testing). (*E*) Effect of the PAR_1-specific antagonist RWJ-58259 on thrombin-induced CCL2 gene expression by A549 cells. Cells were preincubated with RWJ-58259 (2 to 6 μM) or an equivalent dilution of vehicle (DMSO) for 30 minutes before exposure to thrombin for 1.5 hours. CCL2 mRNA levels for each condition were assessed by qPCR. Data are expressed as fold change relative to medium control after normalization to 18S RNA, and represent the mean ± SEM from four replicates per group with each concentration of antagonist. $^{*}P < 0.05$, comparison of thrombin-induced CCL2 ΔCp with CCL2 ΔCp in the presence of vehicle-alone CCL2 ΔCp; $^{\Psi}P < 0.05$, comparison of thrombin-induced CCL2 ΔCp in the presence of antagonist with thrombin-induced ΔCp in the presence of vehicle alone (one-way ANOVA with Student-Newman-Keuls post-hoc testing). (*F*) Effect of the PAR_1-specific antagonist RWJ-58259 on thrombin-induced CCL2 released by A549 cells (thrombin [10 nM], 6 h). Cell supernatants were analyzed for CCL2 protein release by ELISA. Data represent the mean ± SEM of three replicates per group. $^{***}P < 0.001$, comparison of thrombin-induced CCL2 with CCL2 released in the presence of vehicle alone; $^{\Psi\Psi\Psi}P < 0.001$, comparison of thrombin-induced CCL2 in the presence of antagonist, with thrombin-induced CCL2 in the presence of vehicle alone (one-way ANOVA with Student-Newman-Keuls post-hoc testing). Similarly, (*G*) shows the effect of the PAR_1–$G\alpha_q$-specific antagonist, Q94, on thrombin-induced CCL2 release by A549 cells (thrombin [10 nM], 6 h). Cell supernatants were

with primary alveolar type II epithelial cells, freshly isolated from lung resections from patients undergoing surgical resection and from murine lungs. Baseline CCL2 production rates were almost 10-fold higher for primary human and murine epithelial cells compared with A549 cells. Nonetheless, thrombin significantly increased CCL2 release by these primary epithelial cell cultures, with the greatest stimulation (4.4-fold) obtained for murine cells (Figures 6A and 6B).

DISCUSSION

Local activation of the coagulation cascade is characteristically observed in patients with inflammatory and fibrotic lung disorders, including IPF, systemic sclerosis, and ARDS (37). It is generally held that damage to the lung vasculature leads to leak and local activation of coagulation zymogens, such as prothrombin, as a consequence of the local upregulation of tissue factor and the initiation of the extrinsic pathway of coagulation (reviewed in [1]). In support of the *in vivo* pathological relevance of both thrombin and its major signaling receptor PAR_1, we have previously reported that either direct thrombin inhibition or PAR_1 deficiency affords substantial protection from bleomycin-induced lung fibrosis in rodents (2, 7). The protection afforded by PAR_1 deficiency was found to be associated with a marked attenuation in the CCL2 response, suggesting that CCL2 levels are regulated by PAR_1 in experimental lung fibrosis. CCL2 is a potent chemoattractant for inflammatory cells, including monocytes, and has also been implicated in the development of experimental lung fibrosis via its ability to act as a chemoattractant for fibrocytes (13). Moreover, CCL2 may also exert profibrotic effects by inducing the expression of transforming growth factor-β and by down-regulating the production of the major antifibrotic prostaglandin E_2 (38, 39). Defining the mechanisms leading to the induction of CCL2 in fibrotic and fibroproliferative lung disease is therefore of paramount importance in our quest to develop urgently needed novel therapies for this group of disorders.

This study shows for the first time that activation of PAR_1 on the alveolar and bronchial epithelium may represent an important mechanism leading to local CCL2 release in pulmonary fibrosis. First, our studies show extensive coimmunostaining for PAR_1 and CCL2 on both the alveolar and bronchial epithelium in IPF, as well as the bleomycin model of lung injury and fibrosis. Second, gene expression studies of laser-microdissected alveolar septae revealed that PAR_1 and CCL2 are markedly increased at the mRNA level in the alveolar epithelium of patients with IPF compared with control donor lung. Third, we demonstrate that activation of PAR_1 induces the rapid and dramatic expression and release of CCL2 by alveolar and bronchial epithelial cells *in vitro*.

PAR_1 and CCL2 Are Coexpressed in Human and Murine Fibrotic Lungs

Alveolar epithelial cells in the human fibrotic lung, and in particular in IPF, are morphologically abnormal, with hyperplastic pneumocytes and reactive elongated cells overlying fibroblastic foci (19). In response to bleomycin injury, type II alveolar epithelial cells also adopt a hyperplastic activated phenotype (21, 22). The presence of hyperplastic type II cells is a characteristic feature of this model and also of the lungs of patients with ARDS (20).

The major aim of this study was to examine the main cell types that might be responsible for PAR_1-inducible CCL2 in pulmonary fibrosis. We first examined the immunohistochemical localization of PAR_1 and CCL2 in bleomycin-induced lung injury. We report that, in contrast to the weak immunostaining for PAR_1 and CCL2 in saline-instilled control lungs, immunostaining for these proteins was prominent on the airway and alveolar epithelium after bleomycin injury. Analysis of multiple serial sections further led us to conclude that these two proteins are likely coexpressed by these cell types, as well as by infiltrating macrophages.

We next examined the expression of PAR_1 and CCL2 in serial sections from IPF lung. The extensive distortion of the lung architecture in IPF renders the identification of different cell types problematic. We therefore used antibodies against the specific epithelial marker, CK7, and the macrophage-specific marker, CD68, to be able to distinguish the cuboidal bronchial and hyperplastic alveolar epithelium from infiltrating macrophages. These studies revealed that PAR_1 immunoreactivity was restricted to the alveolar and bronchial epithelium as well as resident macrophages in control lungs and that there was no signal for CCL2 in the control lung, apart from on resident macrophages only. In contrast, in the IPF lung, numerous CK7-positive alveolar epithelial cells overlying fibrotic areas were strongly immunoreactive for both PAR_1 and CCL2. The most impressive signal in terms of number of positive cells and intensity of dual staining was observed for the CK7-positive hyperplastic epithelium. The CK7-positive bronchial epithelium bordering fibrotic foci was also positive for both PAR_1 and CCL2 in discrete areas, but the distant ciliated bronchial epithelium expressing CCL2 was completely negative for PAR_1. Additional analysis by dual immunofluorescence confirmed the colocalization of PAR_1 and CCL2 on the alveolar epithelium overlying fibrotic foci. It is worth pointing out that this staining pattern was confined to discrete patches of cells, intensely immunoreactive for both PAR_1 and CCL2 within these areas. Positive immunoreactivity for both antigens was also observed on numerous CD68-positive macrophages, whereas endothelial cells, fibroblasts, and smooth muscle cells were strongly immunoreactive for PAR_1 but were only weakly positive for CCL2.

These colocalization studies led us to hypothesize that the activated epithelium, as well as macrophages, might represent prominent cellular sources of PAR_1-inducible CCL2 in IPF. This notion was further supported by analysis of the expression of PAR_1 and CCL2 by qPCR in alveolar septae obtained by laser microdissection of frozen lung sections. This analysis revealed that PAR_1 and CCL2 mRNA levels are highly upregulated in the alveolar epithelium of patients with IPF compared with control donor lung.

PAR_1 Activation on Lung Epithelial Cells Induces the Expression and Release of CCL2

At the time these experiments were performed, CCL2 was known to be a PAR_1-inducible gene in certain cell types, including macrophages, endothelial cells, and fibroblasts (40–42). However, there was no published evidence that CCL2 might be a PAR_1-inducible gene in lung epithelial cells. We therefore next

analyzed for CCL2 protein release by ELISA. Data represent the mean ± SEM of three replicates per group. ***$P < 0.001$, comparison of thrombin-induced CCL2 with CCL2 released in the presence of vehicle alone; $^{\Psi\Psi\Psi}P < 0.001$, comparison of thrombin-induced CCL2 in the presence of antagonist with that of thrombin-induced CCL2 in the presence of vehicle alone (one-way ANOVA with Student-Newman-Keuls post-hoc testing). (*H*) Effect of the PAR_1-specific antagonist RWJ-58259 on thrombin-induced protein expression (thrombin [10 nM], 1.5 h and release [6 h] from bronchial epithelial cells [BEAS-2B]). Data are expressed and compared as described in (*E*) and (*F*).

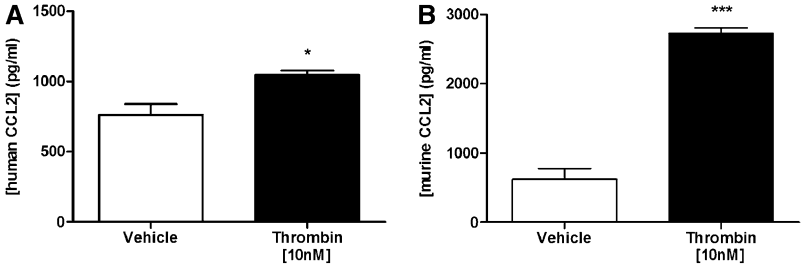

Figure 6. Thrombin induces chemokine (CC motif) ligand-2 (CCL2) release by freshly isolated primary alveolar epithelial cells. Confluent monolayers of primary human (*A*) and murine (*B*) type II epithelial cells were serum-starved for 24 hours and incubated for 6 hours with either control medium or medium containing thrombin (10 nM). Primary human type II cells (*A*) were isolated from lungs of grossly normal appearance after resection for lung carcinoma and the data are representative of the trend obtained for three separate donors, although baseline production levels varied for each donor. Data represent the mean ± SEM of three experimental replicates per group. $*P < 0.05$, $***P < 0.001$, comparison of thrombin-induced CCL2 with CCL2 released in the presence of vehicle alone (Student *t* test).

focused on this question, using the cultured lung epithelial cell lines A549 and BEAS-2B as model cell types for the alveolar and bronchial epithelium, respectively. Despite their tumor origin, A549 cells are widely employed as a representative cell for type II alveolar epithelial cells, and display characteristic phenotypic features, including polygonal morphology, apical microvilli, intracellular lamellar bodies, expression of surfactant proteins, and production of phospholipids (43, 44). A549 cells were found to produce CCL2 constitutively in culture, as has been described previously (45). Thrombin time-course and concentration–response studies further showed that thrombin is a rapid and potent inducer of CCL2 gene expression (within 1.5–3 h) and protein release (within 3 to 6 h) from concentrations as low as 0.1 nM onward. The stimulatory effects of thrombin on CCL2 expression were mimicked with the selective PAR_1 agonist, TFLLR, and were completely inhibited with the selective competitive PAR_1 antagonist, RWJ-58259. Thrombin was also found to induce CCL2 release by BEAS-2B cells and these responses were also completely blocked with RWJ-58259, indicating a major role for PAR_1 in mediating these responses of thrombin in both the bronchial and alveolar epithelium.

PAR_1 belongs to the family of seven-transmembrane G protein–coupled receptors and exerts its pluripotent cellular effects by signaling via the recruitment of several distinct G proteins, including members of the $G\alpha_q$, $G\alpha_i$, and $G\alpha_{12/13}$ subfamilies (1). We have shown that thrombin-induced signaling responses in fibroblasts can be blocked with novel pharmacological agents that target the specific interaction between PAR_1 and the G-protein subunit, $G\alpha_q$ (31). In the current study we found that $G\alpha_q$ blockade with the novel PAR_1 antagonist, Q94, also completely blocked thrombin-induced CCL2 release by A549 cells. These data confirm our findings obtained with the competitive PAR_1 antagonist, RWJ-58259, and further demonstrate that PAR_1-induced CCL2 production in human lung epithelial cells is mediated via PAR_1 coupling to the $G\alpha_q$ pathway. The time course of thrombin-induced CCL2 expression was further typical of an immediate-early gene response as was reported for lung fibroblasts (31), indicating that thrombin exerts its stimulatory effects on CCL2 expression via a direct receptor-mediated mechanism rather than via the release of a secondary mediator, such as IL-1 or tumor necrosis factor-α.

To consolidate our findings with epithelial cell lines, we further confirmed that thrombin also increases CCL2 release by freshly isolated primary human and murine alveolar epithelial cells. Interestingly, basal CCL2 production in primary cells was about 10-fold greater than for A549 cells and the response to thrombin was greater for alveolar epithelial cells of murine origin than for human cells. In comparing the magnitude of induction in CCL2 release obtained in response to thrombin stimulation in this study with that reported for other PAR_1- and CCL2-expressing cells implicated in the development of IPF, the responses obtained in the epithelial cells were found to be within the same range as reported for monocyte-derived macrophages (41) and lung fibroblasts (31). These data suggest that multiple cell types may therefore contribute to CCL2 release after PAR_1 activation in response to lung injury. However, as already mentioned, the IPF immunolocalization studies revealed that although fibroblasts, smooth muscle cells, and endothelial cells were strongly immunoreactive for PAR_1, these cells were relatively weakly immunoreactive for CCL2. In contrast, macrophages were dual immunoreactive for PAR_1 and CCL2 in both control and IPF lungs. Because macrophage recruitment and expansion are commonly observed in numerous fibrotic lung conditions, including IPF, these cells may similarly represent a potential source of PAR_1-inducible CCL2. However, in terms of relative contribution of various cell types to CCL2 release in response to lung injury, it is worth pointing out that studies performed with alveolar macrophages and type II epithelial cells isolated from the same donor lungs demonstrated that CCL2 baseline production rates of type II epithelial cells are about 10-fold higher than those of alveolar macrophages (46).

Epithelial cell CCL2 release experiments were also performed with coagulation factor FXa, which is capable of activating either PAR_1 or PAR_2 (32, 33), depending on the cell type, and unpublished data from our laboratory have shown that the zymogen, FX, is locally upregulated in IPF (C. J. Scotton, M. A. Krupiczojc, R. C. Chambers, unpublished observation). In contrast to thrombin, FXa, when used at concentrations sufficient to induce PAR_1 signaling in human lung fibroblasts (32), did not significantly influence CCL2 mRNA levels in A549 cells. The lack of cell responsiveness to factor Xa may have several explanations. First, unlike thrombin, which interacts with PAR_1 via multiple binding sites, including its anion-binding exosite I (47), Fxa, which lacks such a site, may require additional cofactors, such as tissue factor and coagulation factor VIIa, for efficient cleavage of PAR_1 or PAR_2 (42). Second, there is accumulating evidence that various activators of PAR_1 induce nonidentical cellular responses because they favor the recruitment of different G-protein subunits by a process referred to as "functional selectivity" (42, 48). Elucidating the basis for the lack of CCL2 induction in response to FXa remains an interesting question but is beyond the scope of the current article.

The final issue deserving further consideration centers around the question concerning whether all thrombin-induced CCL2 release by lung epithelial cells is attributable to activation of PAR_1. The near total blockade of thrombin-induced CCL2 release with the two PAR_1 antagonists reported here supports a major role for PAR_1 in mediating this response at a standard concentration of 10 nM of the proteinase. In addition to activating PAR_1, thrombin is also capable of signaling via PAR_4 (reviewed in [1]). However, thrombin has a much lower affinity for PAR_4 and 10- to 100-fold higher concentrations of thrombin are required to activate this receptor compared with PAR_1 (49). Thrombin is also capable of cleaving PAR_3, but

evidence suggests that PAR_3 is a nonsignaling receptor; rather, it acts as a cofactor for efficient presentation of thrombin to PAR_4 at low concentrations of the proteinase (50) and regulates PAR_1 signaling by dimerizing with this receptor (51). However, because A549 cells have previously been shown to respond to PAR_4 activation *in vitro* (25), we examined the effect of the potent PAR_4 agonist peptide, AYPGKF (34), on A549 cell CCL2 gene expression. No induction was observed and A549 cells were further found to be negative for PAR_4 at the mRNA level under the experimental conditions employed in this study. A subsequent study similarly reported that A549 cells do not express PAR_4 (52). We do not understand the basis for these differing reports regarding the ability of A549 cells to express PAR_4, but it is possible that the experimental conditions under which A549 cells are cultured are critical for determining receptor expression by these cells. The lack of PAR_4 expression and responsiveness to potent PAR_4 peptide agonists, in conjunction with the near total blockade of CCL2 induction by thrombin in the presence of the PAR_1 antagonists, RWJ-58259 and Q94, lead us to conclude that PAR_1 is the major signaling receptor involved in mediating thrombin-induced CCL2 expression by these epithelial cells. Our data are further consistent with a report using the PAR_1 antagonist, SCH 79797, although this study reports that this antagonist afforded only partial inhibition of thrombin-induced CCL2 release (53). This may have several potential explanations, but may be explained by differences between the concentrations of thrombin employed in both studies. We specifically chose a maximal concentration of 10 nM thrombin for our PAR_1 antagonist studies, as this is a commonly used concentration and within the physiological range reported in various disease settings (for a review *see* [1]). It is also worth mentioning that SCH 79797 has been reported to exert off-target effects and have a narrow PAR_1-specific therapeutic window (54).

Conclusions

The findings reported in the present study are, to the best of our knowledge, the first to demonstrate a potential role for PAR_1 on the pulmonary epithelium in the induction of the proinflammatory and fibrogenic chemokine CCL2 in the context of fibrotic lung disease. We propose that strategies aimed at blocking the induction of this PAR_1–CCL2 axis may therefore present a novel opportunity for therapeutic intervention. PAR_1 antagonists are being developed as potent antithrombotic agents (reviewed in [1]). The development of such antagonists for use via an inhalational route targeting the lung epithelium may offer promise for interfering with IPF and potentially other acute and chronic forms of inflammatory and fibrotic lung disease characterized by uncontrolled activation of the coagulation cascade.

Conflict of Interest Statement: P.F.M. does not have a financial relationship with a commercial entity that has an interest in the subject of this manuscript. R.H.J. does not have a financial relationship with a commercial entity that has an interest in the subject of this manuscript. C.J.S. does not have a financial relationship with a commercial entity that has an interest in the subject of this manuscript. M.A.K. does not have a financial relationship with a commercial entity that has an interest in the subject of this manuscript. M.K. does not have a financial relationship with a commercial entity that has an interest in the subject of this manuscript. D.C.J.H. does not have a financial relationship with a commercial entity that has an interest in the subject of this manuscript. R.J.M. does not have a financial relationship with a commercial entity that has an interest in the subject of this manuscript. A.D. is employed by Centocor Research and Development, Inc. A.J.T. does not have a financial relationship with a commercial entity that has an interest in the subject of this manuscript. T.D.T. does not have a financial relationship with a commercial entity that has an interest in the subject of this manuscript. O.E. does not have a financial relationship with a commercial entity that has an interest in the subject of this manuscript. R.C.C. received a research funding agreement from Centocor, which funded part of this study.

References

1. Chambers RC. Procoagulant signalling mechanisms in lung inflammation and fibrosis: novel opportunities for pharmacological intervention? *Br J Pharmacol* 2008;153:S367–S378.
2. Howell DC, Goldsack NR, Marshall RP, McAnulty RJ, Starke R, Purdy G, Laurent GJ, Chambers RC. Direct thrombin inhibition reduces lung collagen, accumulation, and connective tissue growth factor mRNA levels in bleomycin-induced pulmonary fibrosis. *Am J Pathol* 2001;159:1383–1395.
3. Yasui H, Gabazza EC, Tamaki S, Kobayashi T, Hataji O, Yuda H, Shimizu S, Suzuki K, Adachi Y, Taguchi O. Intratracheal administration of activated protein C inhibits bleomycin-induced lung fibrosis in the mouse. *Am J Respir Crit Care Med* 2001;163:1660–1668.
4. Gunther A, Lubke N, Ermert M, Schermuly RT, Weissmann N, Breithecker A, Markart P, Ruppert C, Quanz K, Ermert L, *et al.* Prevention of bleomycin-induced lung fibrosis by aerosolization of heparin or urokinase in rabbits. *Am J Respir Crit Care Med* 2003;168: 1358–1365.
5. Kijiyama N, Ueno H, Sugimoto I, Sasaguri Y, Yatera K, Kido M, Gabazza EC, Suzuki K, Hashimoto E, Takeya H. Intratracheal gene transfer of tissue factor pathway inhibitor attenuates pulmonary fibrosis. *Biochem Biophys Res Commun* 2006;339:1113–1119.
6. Hattori N, Degen JL, Sisson TH, Liu H, Moore BB, Pandrangi RG, Simon RH, Drew AF. Bleomycin-induced pulmonary fibrosis in fibrinogen-null mice. *J Clin Invest* 2000;106:1341–1350.
7. Howell DC, Johns RH, Lasky JA, Shan B, Scotton CJ, Laurent GJ, Chambers RC. Absence of proteinase-activated receptor-1 signaling affords protection from bleomycin-induced lung inflammation and fibrosis. *Am J Pathol* 2005;166:1353–1365.
8. Bogatkevich GS, Gustilo E, Oates JC, Feghali-Bostwick C, Harley RA, Silver RM, Ludwicka-Bradley A. Distinct PKC isoforms mediate cell survival and DNA synthesis in thrombin-induced myofibroblasts. *Am J Physiol Lung Cell Mol Physiol* 2005;288:L190–L201.
9. Grandaliano G, Di Paolo S, Monno R, Stallone G, Ranieri E, Pontrelli P, Gesualdo L, Schena FP. Protease-activated receptor 1 and plasminogen activator inhibitor 1 expression in chronic allograft nephropathy: the role of coagulation and fibrinolysis in renal graft fibrosis. *Transplantation* 2001;72:1437–1443.
10. Marra F, DeFranco R, Grappone C, Milani S, Pinzani M, Pellegrini G, Laffi G, Gentilini P. Expression of the thrombin receptor in human liver: up-regulation during acute and chronic injury. *Hepatology* 1998; 27:462–471.
11. Rose CE Jr, Sung SS, Fu SM. Significant involvement of CCL2 (MCP-1) in inflammatory disorders of the lung. *Microcirculation* 2003;10:273–288.
12. Antoniades HN, Neville-Golden J, Galanopoulos T, Kradin RL, Valente AJ, Graves DT. Expression of monocyte chemoattractant protein 1 mRNA in human idiopathic pulmonary fibrosis. *Proc Natl Acad Sci USA* 1992;89:5371–5375.
13. Moore BB, Kolodsick JE, Thannickal VJ, Cooke K, Moore TA, Hogaboam C, Wilke CA, Toews GB. CCR2-mediated recruitment of fibrocytes to the alveolar space after fibrotic injury. *Am J Pathol* 2005;166:675–684.
14. Moore BB, Paine R III, Christensen PJ, Moore TA, Sitterding S, Ngan R, Wilke CA, Kuziel WA, Toews GB. Protection from pulmonary fibrosis in the absence of CCR2 signaling. *J Immunol* 2001;167:4368–4377.
15. Gharaee-Kermani M, McCullumsmith RE, Charo IF, Kunkel SL, Phan SH. CC-chemokine receptor 2 required for bleomycin-induced pulmonary fibrosis. *Cytokine* 2003;24:266–276.
16. Inoshima I, Kuwano K, Hamada N, Hagimoto N, Yoshimi M, Maeyama T, Takeshita A, Kitamoto S, Egashira K, Hara N. Anti-monocyte chemoattractant protein-1 gene therapy attenuates pulmonary fibrosis in mice. *Am J Physiol Lung Cell Mol Physiol* 2004;286:L1038–L1044.
17. Suga M, Iyonaga K, Ichiyasu H, Saita N, Yamasaki H, Ando M. Clinical significance of MCP-1 levels in BALF and serum in patients with interstitial lung diseases. *Eur Respir J* 1999;14:376–382.
18. Goodman RB, Strieter RM, Martin DP, Steinberg KP, Milberg JA, Maunder RJ, Kunkel SL, Walz A, Hudson LD, Martin TR. Inflammatory cytokines in patients with persistence of the acute respiratory distress syndrome. *Am J Respir Crit Care Med* 1996;154: 602–611.
19. Selman M, Pardo A. Role of epithelial cells in idiopathic pulmonary fibrosis: from innocent targets to serial killers. *Proc Am Thorac Soc* 2006;3:364–372.

20. Stanley MW, Henry-Stanley MJ, Gajl-Peczalska KJ, Bitterman PB. Hyperplasia of type II pneumocytes in acute lung injury: cytologic findings of sequential bronchoalveolar lavage. *Am J Clin Pathol* 1992; 97:669–677.
21. Folkesson HG, Nitenberg G, Oliver BL, Jayr C, Albertine KH, Matthay MA. Upregulation of alveolar epithelial fluid transport after subacute lung injury in rats from bleomycin. *Am J Physiol* 1998;275:L478–L490.
22. Karam H, Hurbain-Kosmath I, Housset B. Antioxidant activity in alveolar epithelial type 2 cells of rats during the development of bleomycin injury. *Cell Biol Toxicol* 1998;14:13–22.
23. Imokawa S, Sato A, Hayakawa H, Kotani M, Urano T, Takada A. Tissue factor expression and fibrin deposition in the lungs of patients with idiopathic pulmonary fibrosis and systemic sclerosis. *Am J Respir Crit Care Med* 1997;156:631–636.
24. Bastarache JA, Wang L, Geiser T, Wang Z, Albertine KH, Matthay MA, Ware LB. The alveolar epithelium can initiate the extrinsic coagulation cascade through expression of tissue factor. *Thorax* 2007; 62:608–616.
25. Asokananthan N, Graham PT, Fink J, Knight DA, Bakker AJ, McWilliam AS, Thompson PJ, Stewart GA. Activation of protease-activated receptor (PAR)-1, PAR-2, and PAR-4 stimulates IL-6, IL-8, and prostaglandin E_2 release from human respiratory epithelial cells. *J Immunol* 2002;168:3577–3585.
26. Johns RH, Scotton CJ, Laurent GJ, Chambers RC. PAR1 signalling in lung epithelial cells induces the expression of CCL2/MCP-1 and CTGF [abstract]. *Thorax* 2005;60:ii23.
27. Johns RH, Scotton CJ, Thorley AJ, Laurent GJ, Tetley TD, Chambers RC. PAR1 activation on lung epithelial cells promotes CCL2 expression [abstract]. *Proc Am Thorac Soc* 2006;3:A760.
28. Fink L, Seeger W, Ermert L, Hanze J, Stahl U, Grimminger F, Kummer W, Bohle RM. Real-time quantitative RT-PCR after laser-assisted cell picking. *Nat Med* 1998;4:1329–1333.
29. Thorley AJ, Goldstraw P, Young A, Tetley TD. Primary human alveolar type II epithelial cell CCL20 (macrophage inflammatory protein-3α)-induced dendritic cell migration. *Am J Respir Cell Mol Biol* 2005;32: 262–267.
30. Corti M, Brody AR, Harrison JH. Isolation and primary culture of murine alveolar type II cells. *Am J Respir Cell Mol Biol* 1996;14:309–315.
31. Deng X, Mercer PF, Scotton CJ, Gilchrist A, Chambers RC. Thrombin induces fibroblast CCL2/JE production and release via coupling of PAR1 to Gαq and cooperation between ERK1/2 and Rho kinase signaling pathways. *Mol Biol Cell* 2008;19:2520–2533.
32. Blanc-Brude OP, Archer F, Leoni P, Derian C, Bolsover S, Laurent GJ, Chambers RC. Factor Xa stimulates fibroblast procollagen production, proliferation, and calcium signaling via PAR_1 activation. *Exp Cell Res* 2005;304:16–27.
33. Camerer E, Kataoka H, Kahn M, Lease K, Coughlin SR. Genetic evidence that protease-activated receptors mediate factor Xa signaling in endothelial cells. *J Biol Chem* 2002;277:16081–16087.
34. Henriksen RA, Hanks VK. PAR-4 agonist AYPGKF stimulates thromboxane production by human platelets. *Arterioscler Thromb Vasc Biol* 2002;22:861–866.
35. Visscher DW, Myers JL. Histologic spectrum of idiopathic interstitial pneumonias. *Proc Am Thorac Soc* 2006;3:322–329.
36. Reddel RR, Ke Y, Gerwin BI, McMenamin MG, Lechner JF, Su RT, Brash DE, Park JB, Rhim JS, Harris CC. Transformation of human bronchial epithelial cells by infection with SV40 or adenovirus-12 SV40 hybrid virus, or transfection via strontium phosphate coprecipitation with a plasmid containing SV40 early region genes. *Cancer Res* 1988;48:1904–1909.
37. Idell S, Gonzalez K, Bradford H, MacArthur CK, Fein AM, Maunder RJ, Garcia JG, Griffith DE, Weiland J, Martin TR, *et al.* Procoagulant activity in bronchoalveolar lavage in the adult respiratory distress syndrome: contribution of tissue factor associated with factor VII. *Am Rev Respir Dis* 1987;136:1466–1474.
38. Gharaee-Kermani M, Denholm EM, Phan SH. Costimulation of fibroblast collagen and transforming growth factor β_1 gene expression by monocyte chemoattractant protein-1 via specific receptors. *J Biol Chem* 1996;271:17779–17784.
39. Moore BB, Peters-Golden M, Christensen PJ, Lama V, Kuziel WA, Paine R III, Toews GB. Alveolar epithelial cell inhibition of fibroblast proliferation is regulated by MCP-1/CCR2 and mediated by PGE_2. *Am J Physiol Lung Cell Mol Physiol* 2003;284:L342–L349.
40. Bachli EB, Pech CM, Johnson KM, Johnson DJ, Tuddenham EG, McVey JH. Factor Xa and thrombin, but not factor VIIa, elicit specific cellular responses in dermal fibroblasts. *J Thromb Haemost* 2003;1:1935–1944.
41. Colognato R, Slupsky JR, Jendrach M, Burysek L, Syrovets T, Simmet T. Differential expression and regulation of protease-activated receptors in human peripheral monocytes and monocyte-derived antigen-presenting cells. *Blood* 2003;102:2645–2652.
42. Riewald M, Ruf W. Protease-activated receptor-1 signaling by activated protein C in cytokine-perturbed endothelial cells is distinct from thrombin signaling. *J Biol Chem* 2005;280:19808–19814.
43. Foster KA, Oster CG, Mayer MM, Avery ML, Audus KL. Characterization of the A549 cell line as a type II pulmonary epithelial cell model for drug metabolism. *Exp Cell Res* 1998;243:359–366.
44. Shapiro DL, Nardone LL, Rooney SA, Motoyama EK, Munoz JL. Phospholipid biosynthesis and secretion by a cell line (A549) which resembles type II alveolar epithelial cells. *Biochim Biophys Acta* 1978;530:197–207.
45. Pechkovsky DV, Goldmann T, Ludwig C, Prasse A, Vollmer E, Muller-Quernheim J, Zissel G. CCR2 and CXCR3 agonistic chemokines are differently expressed and regulated in human alveolar epithelial cells type II. *Respir Res* 2005;6:75.
46. Thorley AJ, Ford PA, Giembycz MA, Goldstraw P, Young A, Tetley TD. Differential regulation of cytokine release and leukocyte migration by lipopolysaccharide-stimulated primary human lung alveolar type II epithelial cells and macrophages. *J Immunol* 2007;178:463–473.
47. Myles T, Le Bonniec BF, Stone SR. The dual role of thrombin's anion-binding exosite-I in the recognition and cleavage of the protease-activated receptor 1. *Eur J Biochem* 2001;268:70–77.
48. McLaughlin JN, Shen L, Holinstat M, Brooks JD, Dibenedetto E, Hamm HE. Functional selectivity of G protein signaling by agonist peptides and thrombin for the protease-activated receptor-1. *J Biol Chem* 2005;280:25048–25059.
49. O'Brien PJ, Molino M, Kahn M, Brass LF. Protease activated receptors: theme and variations. *Oncogene* 2001;20:1570–1581.
50. Nakanishi-Matsui M, Zheng YW, Sulciner DJ, Weiss EJ, Ludeman MJ, Coughlin SR. PAR3 is a cofactor for PAR4 activation by thrombin. *Nature* 2000;404:609–613.
51. McLaughlin JN, Patterson MM, Malik AB. Protease-activated receptor-3 (PAR3) regulates PAR1 signaling by receptor dimerization. *Proc Natl Acad Sci USA* 2007;104:5662–5667.
52. Grishina Z, Ostrowska E, Halangk W, Sahin-Toth M, Reiser G. Activity of recombinant trypsin isoforms on human proteinase-activated receptors (PAR): mesotrypsin cannot activate epithelial PAR-1, -2, but weakly activates brain PAR-1. *Br J Pharmacol* 2005;146:990–999.
53. Wang H, Yi T, Zheng Y, He S. Induction of monocyte chemoattractant protein-1 release from A549 cells by agonists of protease-activated receptor-1 and -2. *Eur J Cell Biol* 2007;86:233–242.
54. Di Serio C, Pellerito S, Duarte M, Massi D, Naldini A, Cirino G, Prudovsky I, Santucci M, Geppetti P, Marchionni N, *et al.* Protease-activated receptor 1-selective antagonist SCH79797 inhibits cell proliferation and induces apoptosis by a protease-activated receptor 1-independent mechanism. *Basic Clin Pharmacol Toxicol* 2007;101: 63–69.